Fabrication of Self-Recoverable Flexible and Stretchable Electronic Devices

Yiwei Han, Jingyan Dong*

Department of Industrial Engineering and Systems Engineering, North Carolina State University, Raleigh, N.C., 27695, U.S.

* Corresponding author. Tel.: +1-919-515-7196
E-mail address: jdong@ncsu.edu

Abstract

In this paper, we developed an EHD printing process for the fabrication of high-resolution self-recoverable flexible and stretchable electronics using low-melting-point metal inks. Three different metal inks were tested for their printability on four different substrates separately to demonstrate the capability of EHD printing technology. EHD printing enables low-cost direct fabrication of metallic conductors with sub-50μm resolution, which represents a promising way to create electronic features with metallic conductivity and excellent flexibility and stretchability. When properly designed, the EHD printed electronics provided a stable resistance under hundreds of bending cycles and many stretching and releasing cycles with high tensile strain, which demonstrates their good flexibility and stretchability in electronics applications. The printed electronics was capable of self-healing under low temperature treatment to recover from failures without sacrificing its electrical properties. Moreover, a high-resolution capacitive sensor array was designed and fabricated. A Finite Element Analysis (FEA) model was developed to study the performance of the designed touch sensor. The results from FEA model agreed well with experimental results, which demonstrated the high-resolution capability of the EHD printing for the direction fabrication of flexible and stretchable devices.

Keywords: Electrohydrodynamic (EHD) printing; metal printing; printing electronics; flexible and stretchable electronics; self-recoverable

1. Introduction

Printing is a powerful tool to fabricate electronics. Current printing technologies that were used in fabricating electronics include inkjet printing[1,2], 3D printing[3-6], direct writing[7-9], dry printing[10], spray coating[11,12], spin coating[13], screen printing[14], dual-trans printing[15] and soft lithography[16]. A variety of the materials have been used in those printing technologies, such as conductive polymers [10,17], metal nanoparticles/nanowire [18-

20], carbon tube [21,22], and liquid metal or low melting point metal [4,8,23,24]. Those materials offer good performance for their specific electronics application. However, many limitations still existed, for example, the electronics printed with polymers doesn't have very good conductivity; electronics printed with metal nanoparticle/nanowire need to perform post-process to improve its conductivity; liquid metal can offer good conductivity and self-healing property [25,26], but it is very expensive comparing with materials mentioned above, and the resolution of the printed features is generally at millimetre scale and packaging is needed to protect the devices. With those limitations, most of those printing technologies cannot offer both high-resolution and high conductivity in electronics. Only a few printing technologies, for example, soft lithography based contact printing can provide high resolution, but the fabrication process is very complex and molds/masks are generally needed, which increase the time and cost of the overall manufacturing process.

Electrohydrodynamic (EHD) is a cost-effective, high-resolution printing method [27-29], which can produce fine droplet or jet that have much smaller size than the nozzle dimension by inducing electric field to the printing system. Many materials have already be applied to EHD printing, such as polymeric materials[30,31], biomaterials[32], metal nanoparticles[33], and some studies [34-36] have demonstrated the capability of fabricating electronics with EHD printing. However, to the best of our knowledge, no study has been reported on direct EHD printing of molten metal inks for the fabrication of electronic devices.

In this work, we studied the fabrication of flexible and stretchable electronics by direct EHD printing of molten metal inks. Micro-scale metallic electronics were successfully fabricated with sub-50μm resolution and without performing any post-processing. The printed electronic features were tested under cyclic bending test and stretching tests, and the results demonstrated excellent flexibility after hundreds of bending cycles with a bending radius of 10mm, and during stretching/releasing cycles with a large tensile strain of 70%. Moreover, the printed electronic devices were capable of recovering from failure by heating the sample above the eutectic temperature of the metal ink and applying a small pressure. The EHD printed molten metal features provides a promising method for mask-less fabrication of electronics with metallic conductivity, excellent flexibility and stretchability, and capability of self-recovery.

2. Characterization of EHD Printing Process

The EHD printing system consists four subsystems: pneumatic dispensing system, thermal control system, high voltage supply system, and precision three-axis motion system. Figure 1 (a) shows the schematic of the EHD printing system setup. The pneumatic dispensing system is controlled by a pressure regulator that provides a small pressure (0.1psi) to assist the ink flow to the nozzle tip. The thermal control system includes heating rope, thermocouple, and a PID controller that can provide a maximum temperature of 400°C to the

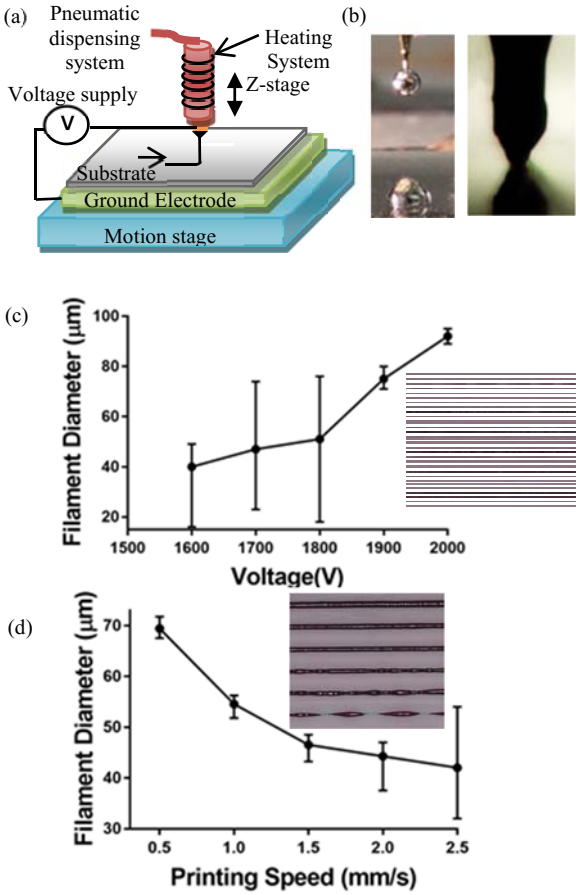

Fig. 1.(a) Schematic of EHD printing system. (b) Droplet printed by extrusion method (left) and cone shape (right) of EHD metal printing. (c) The diameter of printed metallic filaments on glass slide at different voltages of 500, 1600, 1700, 1800, 1900, and 2000V with a constant speed of 0.5mm/s. (d) Printed metallic filaments on glass slide at printing speeds of 0.5, 1, 1.5, 2, 3, 4mm/s with a constant printing voltage of 1900V.

system. The printing nozzle and the ground electrode are connected to a high-voltage supply, which can provide a maximum voltage of 10K volts. The precision motion stage has three linear stages in XYZ direction with a repeatability and accuracy of 100nm. A high-resolution camera is used to monitor the printing process. The printing nozzle with an inner diameter of 160μm is used for EHD printing. The low-melting-point metal inks used in this study are Field's Metal (32.5% Bismuth, 51% Indium, 16.5% Tin), Wood's Metal (50% Bismuth, 13.3% Tin, 26.7% Lead, and 10% Cadmium), and solder (32% Bismuth, 48% Tin, 20% Lead). Four different types of substrates, glass slide, PDMS, PET, and photo paper are used in this study to show the capability of EHD printing onto different substrates.

In EHD printing of molten metal, a voltage is applied to the system to provide the electrostatic force to eject ink out from the nozzle. When the applied voltage is larger enough, only a very small pressure is needed to keep the ink flow rate. In this study, a pressure of 0.1psi is applied to the system. Figure 1 (b) compares the printing behaviors between direct extrusion based printing and EHD printing. It clearly shows that the diameter of the ejected droplet in direct extrusion is much larger than the nozzle size. However, for EHD printing, the formed cone shape and ejected filament have a smaller size than the nozzle diameter, which can print high resolution features.

The printing voltage and printing speed are the two critical printing parameters for EHD direct metal printing because both of them affect the printing resolution and the quality of the printed patterns. To find the feasible printing conditions for EHD direct metal printing, characterization experiments for Field's metal were conducted. Figure 1 (c) shows the printing results under different voltages (500V, 1600V, 1700V, 1800V, 1900V, and 2000V respectively from top to bottom) on the glass slides with a constant printing speed of 0.5mm/s. During the EHD printing, the electrostatic force overcomes the viscose force and surface tension force to eject ink out from the nozzle. Insufficient voltage (less than 1600V) brings relatively low ink flow rate that results in discontinuous filaments as in the first line from the top in Figure 1 (c). At 1600V, continous filaments are printed but with limited uniformity, indicating that the ink flow rate is still low and a larger voltage is needed to improve the printing quality. When the voltage is increased to 1900V, uniform and the continuous filament is printed on the substrate. Increasing the voltage increases the ink flow rate. With a constant printing speed, filament printed under higher voltage has a larger line width as shown in the Figure 1 (c). Besides the applied voltage, printing speed also affects the printing behavior. When selecting a constant voltage, the printing system has a constant ink flow rate. Printing speed that is much less than the flow rate results in a large amount of ink collecting around the nozzle and a larger line width. On the other hand, too faster printing speed results in discontinuous or nonuniformity line. In a proper printing speed range, higher printing speed produces a continuous filament with smaller linewidth, which can be easily explained as the tensile strength of the printed filament can hold the filament from being torn apart that allows fewer materials printed in a unit length under higher printing speed condition. Figure 1(d) shows the printing result under different printing speed (0.5, 1, 1.5, 2, 3, 4mm/s) using a constant voltage of 1900V. When the printing speed is 1.5mm/s, good uniformity filaments with linewidth of about 45μm are successfully printed.

Besides printing Field's metal on glass, EHD printing is capable of printing a variant of metal inks onto different substrates. To demonstrate the capability of EHD printing of different materials onto different substrates, three different low-melting-point metal inks (Field's metal, Wood's metal and solder) and four different substrates (PDMS, PET, and photo paper) are selected to perform the experiment. Field's metal, Wood's metal, and solder are all eutectic alloys with the melting point of 60 °C, 70 °C, and 160°C respectively. Due to the different melting points of printing materials, the printing temperatures are selected to 175°C for Field's metal and Wood's metal, and 300°C for the solder to ensure the good ink flowability. For printing onto different substrates, the printing voltage and printing speed have to be adjusted accordingly to achieve reliable printing behaviors, because different substrates have different permittivity, which will affect electric field strength around the nozzle tip. However, the overall effect of the printing voltage and printing speed on the printing behavior is similar to that present in Figure 1. In our study, all three inks have successfully printed on the four different substrates that are widely used in flexible and stretchable electronics. The wettability of the molten metal inks on the substrate affects the adhesion between the printed ink and the substrate

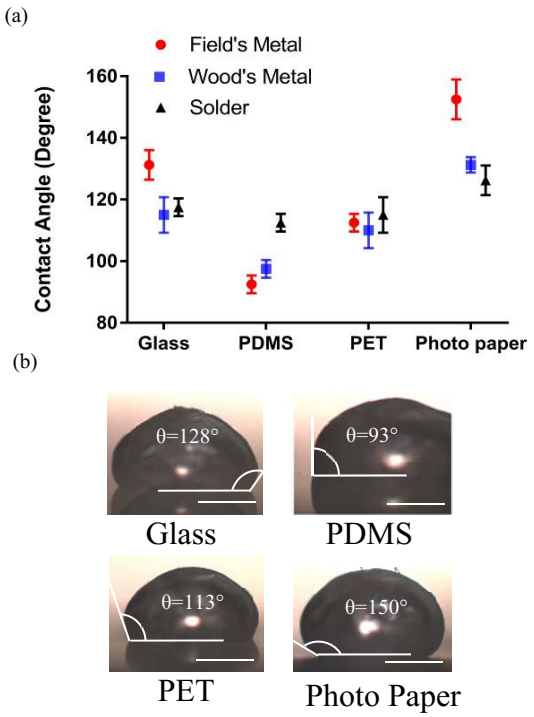

Fig. 2. (a) Contact angles for three molten metal inks on four different substrates. (b) Optical image for measuring the contact angle of Field's metal droplet on different substrates. (Scale bar: 500μm)

thus affect the printing performance. The wettability of three metal inks on four substrates was studied by measuring the contact angle between the interface of ink and substrate surface. The contact angle is measured by evaluating the drop image on the substrate, and the results are shown in Figure 2. From the results, PDMS has the smallest contact angle, which indicated a good wettability and adhesion between PDMS and the metallic ink. Photo paper has the largest contact angle, which indicated a poor adhesion and wettability. These results showed the PDMS has stronger adhesion than the photo paper on the same substrate, which explain that the metallic lines are difficult to be separate from PDMS surface without breaking the lines, but the metallic lines pattern can be easily peeled off from photo paper.

3. Flexibility and Stretchability of EHD Printed Electronics

Among the three metal inks discussed above, Field's metal is lead-free, which is environment-friendly. Thus Field's metal is selected for the device fabrication. EHD printed micro-scale patterns can be

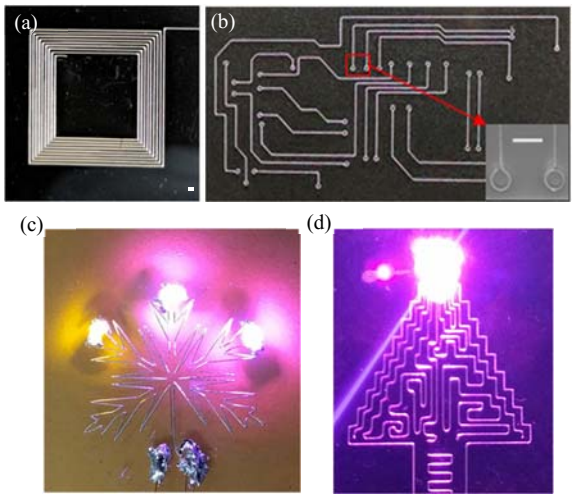

Fig. 3. EHD printed electronics (a) antenna (b) Printed circuit board (c) and (d) optical pattern for other printed electronics. Scale bar: 500μm

used to fabricate electronic devices with good conductivity, flexibility, and stretchability. Figure 3 shows the EHD printed antenna, printed circuit board, and other electronics with a typical linewidth of 50μm. It clearly indicates the capability of using fabricate high-resolution and complex microscale electronics.

To test the flexibility of the printed conductor, a tree leaf pattern was designed and printed on a PDMS film. After necessary wiring, second layer of PDMS is coated on the top of the pattern to secure the pattern from damaging and detaching from the substrate. Figure 4 shows the printed pattern that connected a battery to light a LED at bending state. To test its flexibility, a bending test is performed on a bending machine. The printed pattern is bent at diameter ranging from 19mm to 5mm, and a multimeter is used to measure the resulting resistance of the pattern. Figure 4 shows the bending result that the resistance

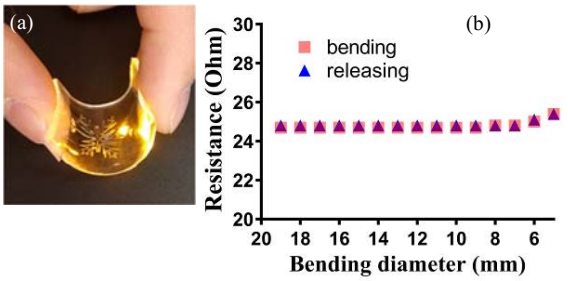

Fig. 4.(a) EHD printed leaf pattern remained conductive at the bending state, which the LED is still ON during the bending. (b) Resistance of the conductor as a function of bending diameter.

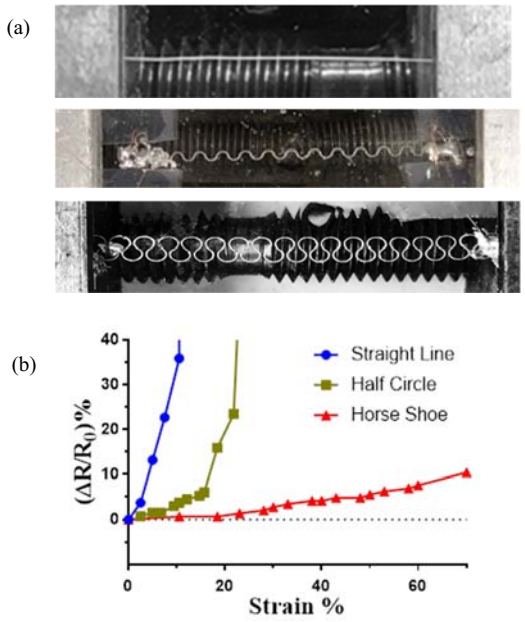

Fig. 5. (a) Optical image of printed different conductor pattern (from top to bottom: a straight-line. Half circle pattern and horseshoe pattern. (b) Resistance change as a function of tensile strain (0–70%) for three different metal pattern.

kept at a constant value when the bending diameter is larger than 7 mm. Even when the bending diameter is reduced to 5mm, the resistance only increases 2.8% from 24.7 Ω to 25.4 Ω. The reason for the changing resistance during the bending test comes from the deformation of the pattern during bending. The strain on the conductor reduced the cross-section area and increased the length, which results in increase of resistance. A small strain causes elastic deformation, which allows the pattern recover to original shape when the strain is released. Moreover, a repetitive bending test (i.e. fatigue test) is performed to study the durability of the printed devices. For the bending diameter of 10mm, the resistance of the pattern barely changed after 1000 bending cycles. The results from Figure 4 shows a good flexibility of the EHD printed metallic features.

To test the stretchability of printed conductors, different metallic patterns (straight line, half circle wave line and a horseshoe pattern [37]) were designed and printed. The sample was clamped on a stretching table, which can provide a continuous strain (Figure 5 (a)). The resistance of the samples with different patterns at different stretching levels is measured by a multimeter. For straight line patten, the maximum

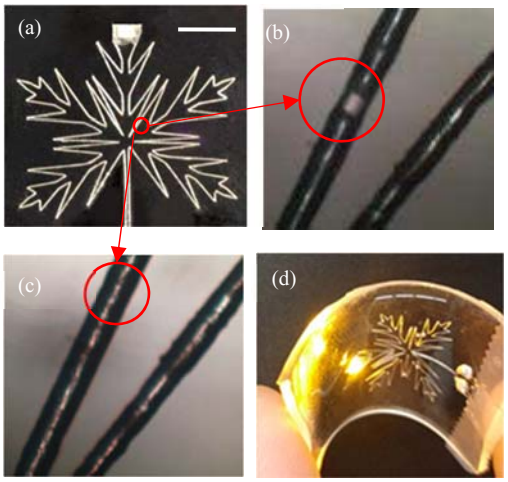

Fig. 6. (a) EHD printed metallic leaf pattern conductor that connected a battery to a LED. The conductor was intentionally broken by overstretching. (b) Optical photograph of a failure (broken connection) in the conductive path. (c) Optical image of the healed failure with the broken gap reconnected. (d) Healed conductor remained conductive when bended by hand. Scale bar: 5mm.

tensile strain is about 10%, which is limited by the the material property of the ink. For the half circle pattern, the maximum tensile strain can reach to 22%, which can be explained that the half circle pattern has a small deformation, and can absorb some strain during the stretching process. To maximize absorbing the tensile strain, a horseshoe pattern is applied to achieve the better stretching performance, because the horseshoe pattern allows to have more deforamation during the stretching before the filament reach to its ultimate tensile strength. The stretching result for three different patterns is shown in the Figure 5. With a horseshoe pattern, the printed feature has a good stretchability, and the resistance only increased about 13% with a 70% tensile strain. Upon release of the strain, the resistance is almost fully recovered and decreased back to original value when the PDMS is fully released. More stretching/releasing cycles in the strain range of 0–70% were performed, and similar response in the resistance was observed. The change in resistance also comes from the changing of cross-section and length of the metal filaments.

Since Filed's metal has a low melting point of 60°C, which is harmless for most of the polymeric substrates used in flexible and stretchable electronics, electronic devices printed with this material are capable of self-healing, which can recover from failure or breakage by a heat treatment of the sample above the eutectic

temperature of the metal ink and a little pressure to the failure point. The heat treatment can melt the metal features encapsulated in the PDMS film, and reconnected the metallic pattern to fix the failure of the conductor. Figure 6 shows a leaf pattern that is used to power a LED. To test the self-healing property, the printed leaf pattern is broken on purpose by applying a tremendous strain. One of the breakpoints is highlighted in Figure 6 (b) and the LED is completely off. Then a heat treatment and a slight pressure are applied to the sample around the breakpoint to help the molten metal flow in the channel. After the healing procedure, the circuit recovered from the failure, and the LED was lighted again. The broken gap in the conductor was connected together, and the failure was healed, as shown in Figure 6(c). The healed sample remained conductive and worked well when it was bent as shown in Figure 6(d).

4. Design and Fabrication of High-Density Touch Sensor Array

To demonstrate high-resolution direct patterning capability of EHD printing, a high-density, and high-resolution touch sensor array is designed and fabricated. The schematic structure of the touch panel with an array of touch nodes is shown in Figure 7 (a). This high-density capacitive touch sensor array is formed by two layers of printed metal filament grid and each intersection of the grid is a sensing point. The sensing mechanism is based on disturbing the fringing electric field by a finger or touching tip, which will bring the capacitance change at the intersection points. The capacitance changes at different points can be used to differentiate which point is touched intentionally. With the high-resolution EHD printing, a 20 x 20 matrix or 400 touch sensors were printed

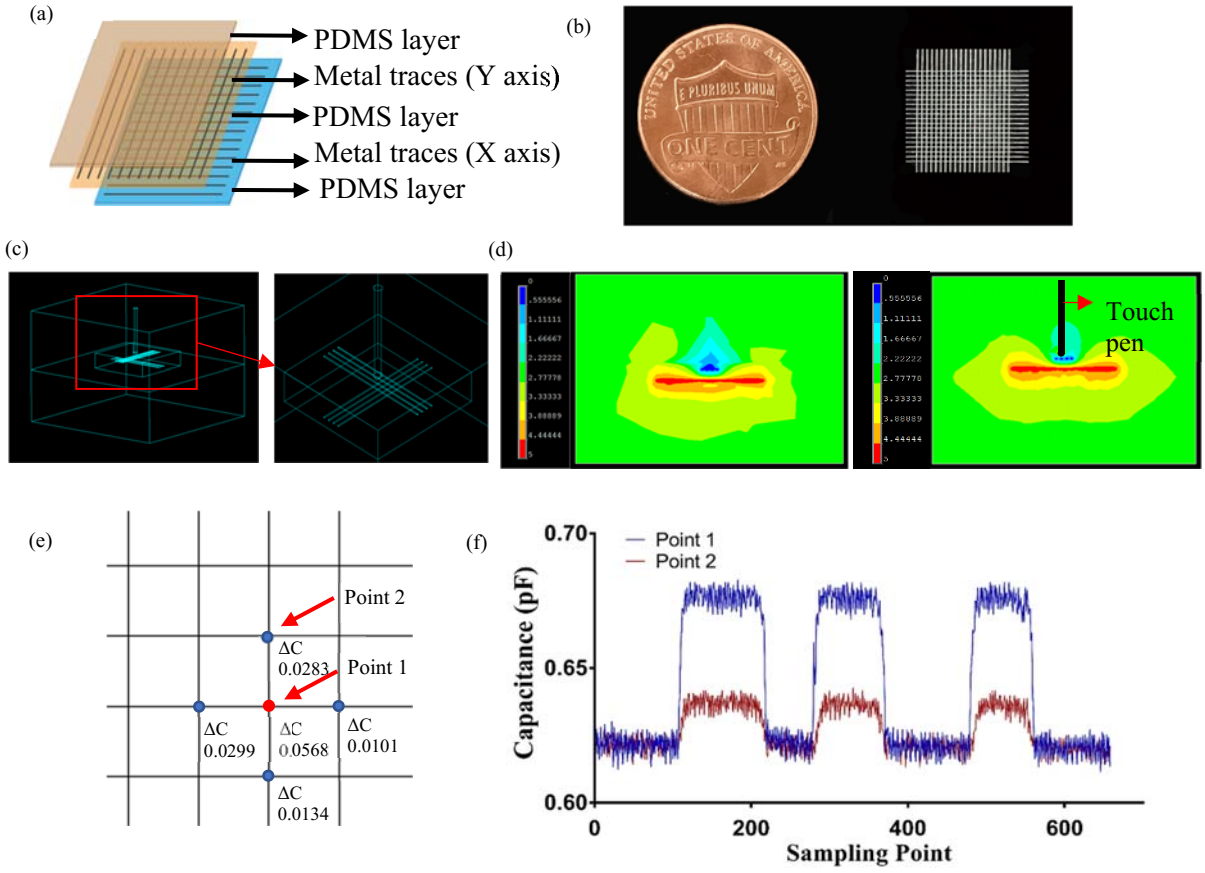

Fig. 7. (a) Schematic of printed projected capacitive touch sensor array. (b) Optical images of a 20x20 touch sensor array. (c) FEA model for touch sensor design. (d) Cross section of electric potential of touch sensor with and without a touch pen (e)Simulation result of the changing capacitance (ΔC) of points when the touch pen touch red point (unit: pF). (f) Change in the capacitance for three touches from the primary touch sensor and a surrounding touch sensor.

onto a 10x10 mm area on a PDMS film. The spacing between two adjacent traces of the metal filaments is 500 microns. Figure 7 (b) shows the optical image of the printed touch sensor array comparing with one cent. The high-resolution printing of high-quality metallic filament can help to minimize the variation in the capacitance from each sensing element.

To study the response of the touch sensor, a FEA model is developed for the touch sensor array with two layers of metal filament grid embedded in PDMS, and a simulation is performed. The model also includes a touch pen as shown in Figure 7 (c) to study the capacitance change when touched. In order to simplify the calculation time, only four metal filaments in each layer are included in the model, which form a 4 x 4 matrix or a 16 touch sensor points. The gap between X-axis metal traces and Y-axis metal traces is 1mm. The thickness of two PDMS layers above and below the metal trace is set to 1.25mm. The FEA simulation results of the electric potential of the touch sensor with and without touch pen are shown in the Figure 7 (d). It is clearly showing that there is a changing of electric potential distribution when the touch pen touches the touch sensor from the top, which is due to the changing dielectric constant around the touch sensor. Figure 7 (e) shows the capacitance change of the points around the touched point using touch tip. From the FEA results, the touched point has a capacitance change more than two times than other points around it, which makes this touch signal detectable and differentiable using the measuring device.

To verify the FEA results and test the performance of the printed touch sensors, while reducing the complexity of electronic connections, a 4x4-sensor array is randomly selected and tested. The 4x4 matrix of touch sensors are connected to a microcontroller board (ARDUINO MEGA 2560) to measure the capacitance change on different nodes. The signal from the touch sensor array is used to control the operation of a 4x4 LED matrix to display the point that is touched by the touch pen. When a sensing point is touched, a single will send to chipboard to be used to control On/Off of the LED. Due to the high density of the touch sensor array, when touching one sensor (i.e. one intersection of the grid), the sensing point around this touched point will also have capacitance change, but with a smaller amplitude. Figure 7 (f) shows the measured result of capacitance changes when touching one point. When one touch sensor is touched by a touch pen tip, which has a tip diameter of 0.7mm, the capacitance of that touch sensor is changed by 0.06pF from 0.62pF to 0.68pF, which is close to the FEA simulation result. The capacitance of the around touch sensor also changes by a smaller amount of 0.02 pF (from 0.62pF to 0.64pF). The difference between experiment result and FEA result may be caused by interference by the environment, wiring, and measuring error. With proper selecting of the threshold value of the capacitance change (0.04 pF in this experiment), only the desired touch sensor is recognized as the touch site, which a signal can be sent to light the corresponding LED.

5. Conclusion

In this study, we successfully developed an EHD printing process for the fabrication of high-resolution flexible and stretchable electronics. The EHD printed electronics have a resolution of less than 50 μm with excellent flexibility and stretchability. A stable electrical response is achieved during the bending test, and the resistance only has a slight change from the rigorous bending. Different pattern designs are studied for the stretchability test, and a horseshoe pattern provides the best stretchability that can withstand a large tensile strain of 70%. Moreover, the printed electronics are capable of self-healing due to the low melting metal ink. With a heat treatment and a small pressure, the electronics can recover from failure without degrading much of their electrical properties. A high-density touch sensor array is designed and fabricated to demonstrate high-resolution direct patterning capability of EHD printing. An FEA model is developed to simulate the touch sensor performance, and compared with experimental results. The experimental results agrees well with the FEA results. With an excellent flexibility, stretchability, self-healing, and high-resolution printing ability, EHD printed electronics can be applied to a variant of applications in wearable device that requires good flexibility and stretachability.

Acknowledgements

This work was supported in part by the National Science Foundation under Grant CMMI-1333775, CBET-1344618, and CMMI-1728370.

References

[1] Ko, S. H., Pan, H., Grigoropoulos, C. P., Luscombe, C. K., Fréchet, J. M., & Poulikakos, D. (2007). All-inkjet-printed

flexible electronics fabrication on a polymer substrate by low-temperature high-resolution selective laser sintering of metal nanoparticles. *Nanotechnology, 18*(34), 345202.

[2] Sirringhaus, H., Kawase, T., Friend, R., Shimoda, T., Inbasekaran, M., Wu, W., & Woo, E. (2000). High-resolution inkjet printing of all-polymer transistor circuits. *Science, 290*(5499), 2123-2126.

[3] Salvo, P., Raedt, R., Carrette, E., Schaubroeck, D., Vanfleteren, J., & Cardon, L. (2012). A 3D printed dry electrode for ECG/EEG recording. *Sensors and Actuators A: Physical, 174*, 96-102.

[4] Ladd, C., So, J. H., Muth, J., & Dickey, M. D. (2013). 3D printing of free standing liquid metal microstructures. *Advanced Materials, 25*(36), 5081-5085.

[5] Muth, J. T., Vogt, D. M., Truby, R. L., Mengüç, Y., Kolesky, D. B., Wood, R. J., & Lewis, J. A. (2014). Embedded 3D printing of strain sensors within highly stretchable elastomers. *Advanced Materials, 26*(36), 6307-6312.

[6] Leigh, S. J., Bradley, R. J., Purssell, C. P., Billson, D. R., & Hutchins, D. A. (2012). A simple, low-cost conductive composite material for 3D printing of electronic sensors. *PloS one, 7*(11), e49365.

[7] Russo, A., Ahn, B. Y., Adams, J. J., Duoss, E. B., Bernhard, J. T., & Lewis, J. A. (2011). Pen-on-paper flexible electronics. *Advanced Materials, 23*(30), 3426-3430.

[8] Boley, J. W., White, E. L., Chiu, G. T. C., & Kramer, R. K. (2014). Direct writing of gallium-indium alloy for stretchable electronics. *Advanced functional materials, 24*(23), 3501-3507.

[9] Wang, L., & Liu, J. (2014). *Printing low-melting-point alloy ink to directly make a solidified circuit or functional device with a heating pen.* Paper presented at the Proceedings of the Royal Society of London A: Mathematical, Physical and Engineering Sciences.

[10] Blanchet, G. B., Loo, Y.-L., Rogers, J., Gao, F., & Fincher, C. (2003). Large area, high resolution, dry printing of conducting polymers for organic electronics. *Applied Physics Letters, 82*(3), 463-465.

[11] Azarova, N. A., Owen, J. W., McLellan, C. A., Grimminger, M. A., Chapman, E. K., Anthony, J. E., & Jurchescu, O. D. (2010). Fabrication of organic thin-film transistors by spray-deposition for low-cost, large-area electronics. *Organic Electronics, 11*(12), 1960-1965.

[12] Cui, Z., Poblete, F. R., Cheng, G., Yao, S., Jiang, X., & Zhu, Y. (2015). Design and operation of silver nanowire based flexible and stretchable touch sensors. *Journal of materials research, 30*(1), 79-85.

[13] Meyer, J., Khalandovsky, R., Görrn, P., & Kahn, A. (2011). MoO3 Films Spin-Coated from a Nanoparticle Suspension for Efficient Hole-Injection in Organic Electronics. *Advanced Materials, 23*(1), 70-73.

[14] Pardo, D. A., Jabbour, G. E., & Peyghambarian, N. (2000). Application of screen printing in the fabrication of organic light-emitting devices. *Advanced Materials, 12*(17), 1249-1252.

[15] Wang, Q., Yu, Y., Yang, J., & Liu, J. (2015). Fast fabrication of flexible functional circuits based on liquid metal dual-trans printing. *Advanced Materials, 27*(44), 7109-7116.

[16] Gozen, B. A., Tabatabai, A., Ozdoganlar, O. B., & Majidi, C. (2014). High-Density Soft-Matter Electronics with Micron-Scale Line Width. *Advanced Materials, 26*(30), 5211-5216.

[17] Forrest, S. R. (2004). The path to ubiquitous and low-cost organic electronic appliances on plastic. *Nature, 428*(6986), 911-918.

[18] Wei, C., Qin, H., Ramírez-Iglesias, N. A., Chiu, C.-P., Lee, Y.-s., & Dong, J. (2014). High-resolution ac-pulse modulated electrohydrodynamic jet printing on highly insulating substrates. *Journal of Micromechanics and Microengineering, 24*(4), 045010.

[19] Qin, H., Cai, Y., Dong, J., & Lee, Y.-S. (2017). Direct Printing of Capacitive Touch Sensors on Flexible Substrates by Additive E-Jet Printing With Silver Nanoinks. *Journal of Manufacturing Science and Engineering, 139*(3), 031011.

[20] Leem, D. S., Edwards, A., Faist, M., Nelson, J., Bradley, D. D., & de Mello, J. C. (2011). Efficient organic solar cells with solution-processed silver nanowire electrodes. *Advanced Materials, 23*(38), 4371-4375.

[21] Cao, Q., Kim, H.-s., Pimparkar, N., Kulkarni, J. P., Wang, C., Shim, M., . . . Rogers, J. A. (2008). Medium-scale carbon nanotube thin-film integrated circuits on flexible plastic substrates. *Nature, 454*(7203), 495-500.

[22] LeMieux, M. C., Roberts, M., Barman, S., Jin, Y. W., Kim, J. M., & Bao, Z. (2008). Self-sorted, aligned nanotube networks for thin-film transistors. *Science, 321*(5885), 101-104.

[23] Han, Y., & Dong, J. (2017). High-Resolution Electrohydrodynamic (EHD) Direct Printing of Molten Metal. *Procedia Manufacturing, 10*, 845-850.

[24] Zheng, Y., He, Z.-Z., Yang, J., & Liu, J. (2014). Personal electronics printing via tapping mode composite liquid metal ink delivery and adhesion mechanism. *Scientific reports, 4*, 4588.

[25] Liu, Y., Gao, M., Mei, S., Han, Y., & Liu, J. (2013). Ultra-compliant liquid metal electrodes with in-plane self-healing capability for dielectric elastomer actuators. *Applied Physics Letters, 103*(6), 064101.

[26] Palleau, E., Reece, S., Desai, S. C., Smith, M. E., & Dickey, M. D. (2013). Self-healing stretchable wires for reconfigurable circuit wiring and 3D microfluidics. *Advanced Materials, 25*(11), 1589-1592.

[27] Park, J.-U., Hardy, M., Kang, S. J., Barton, K., Adair, K., kishore Mukhopadhyay, D., . . . Georgiadis, J. G. (2007). High-resolution electrohydrodynamic jet printing. *Nature materials, 6*(10), 782-789.

[28] Mishra, S., Barton, K. L., Alleyne, A. G., Ferreira, P. M., & Rogers, J. A. (2010). High-speed and drop-on-demand printing with a pulsed electrohydrodynamic jet. *Journal of Micromechanics and Microengineering, 20*(9), 095026.

[29] Poellmann, M. J., Barton, K. L., Mishra, S., & Johnson, A. J. W. (2011). Patterned hydrogel substrates for cell culture with electrohydrodynamic jet printing. *Macromolecular bioscience, 11*(9), 1164-1168.

[30] Han, Y., Wei, C., & Dong, J. (2014). Super-resolution electrohydrodynamic (EHD) 3D printing of micro-structures using phase-change inks. *Manufacturing Letters, 2*(4), 96-99.

[31] Wei, C., & Dong, J. (2014). Development and modeling of melt electrohydrodynamic-jet printing of phase-change inks for high-resolution additive manufacturing. *Journal of Manufacturing Science and Engineering, 136*(6), 061010.

[32] Wei, C., & Dong, J. (2013). Direct fabrication of high-resolution three-dimensional polymeric scaffolds using electrohydrodynamic hot jet plotting. *Journal of Micromechanics and Microengineering, 23*(2), 025017.

[33] Wei, C., Qin, H., Chiu, C.-P., Lee, Y.-S., & Dong, J. (2015).

Drop-on-demand E-jet printing of continuous interconnects with AC-pulse modulation on highly insulating substrates. *Journal of Manufacturing Systems*(37), 505-510. id transparent electrode prepared by electrohydrodynamic (EHD) jet printing. *Journal of Physics D: Applied Physics, 46*(15), 155103.

[34] Lee, S., Kim, J., Choi, J., Park, H., Ha, J., Kim, Y., . . . Paik, U. (2012). Patterned oxide semiconductor by electrohydrodynamic jet printing for transparent thin film transistors. *Applied Physics Letters, 100*(10), 102108.

[35] Lee, D.-Y., Shin, Y.-S., Park, S.-E., Yu, T.-U., & Hwang, J. (2007). Electrohydrodynamic printing of silver nanoparticles by using a focused nanocolloid jet. *Applied Physics Letters, 90*(8), 081905.

[36] Gonzalez, M., Axisa, F., Bulcke, M. V., Brosteaux, D., Vandevelde, B., & Vanfleteren, J. (2008). Design of metal interconnects for stretchable electronic circuits. *Microelectronics Reliability, 48*(6), 825-832.